Colloid Polym Sci 277:1033–1040 (1999)

ORIGINAL CONTRIBUTION

Calorimetric study of the conformational relaxation times in polystyrene

M. Salmerón
C. Torregrosa
A. Vidaurre
J.M. Meseguer Dueñas
M. Monleón Pradas
J.L. Gómez Ribelles

Received: 22 February 1999
Accepted in revised form: 11 June 1999

M. Salmerón · M. Monleón Pradas
J.L. Gómez Ribelles (✉)
Universidad Politécnica de Valencia
Departmento de Termodinámica Aplicada
Camino de Vera s/n
E-46071 Valencia, Spain

C. Torregrosa · A. Vidaurre
J.M. Meseguer Dueñas
Universidad Politécnia de Valencia
Departmento de Física Aplicada
Camino de Vera s/n
E-46071 Valencia, Spain

Abstract The temperature dependence of the relaxation times of the structural relaxation process of polystyrene is determined by temperature-modulated differential scanning calorimetry (TMDSC) and by conventional differential scanning calorimetry (DSC) in the latter by modelling the experimental heat capacity curves measured in heating scans after different thermal histories. The good agreement between both measuring techniques in the temperature interval just above the glass-transition temperature is a guide for the interpretation of the results of the TMDSC technique in the glass-transition region. In addition, the same model applied to DSC scans is used to simulate the TMDSC experiment and the calculated response is compared with the measured scans.

Key words Glass transition · Differential scanning calorimetry · Temperature-modulated differential scanning calorimetry · Polystyrene · Heat capacity

Introduction

When a liquid in equilibrium at a temperature T is subjected to a sudden (instantaneous) change of temperature to T', its thermodynamical (and other physical) properties experience an instantaneous change followed by a relaxation response that takes the material to the new equilibrium state at the temperature T'. This relaxation is caused, in the case of polymer materials, by the conformational rearrangements of the chain segments. The instantaneous response of the material is called the glassy response, and the delayed process is called structural relaxation. The study of the kinetics of the structural relaxation gives information on the conformational mobility, and so it is important to determine the temperature and structure dependence of the characteristic relaxation time.

Conventional differential scanning calorimetry (DSC) is a useful tool to obtain a characterisation of the structural relaxation phenomenon because of the use of small samples, thus with small thermal gradients inside them, and of the great accuracy in the thermal profile of the experiments. Nevertheless DSC is not able to measure directly the relaxation times of the process because it is not possible to measure the evolution of the enthalpy during the isothermal relaxation process. Instead, the specific heat capacity of the sample as a function of the temperature measured in heating scans after different histories has to be integrated to obtain enthalpy data.

A different approach is to elaborate a model in which the evolution of the enthalpy, the configurational entropy, or the fictive temperature is determined assuming a certain dependence of the relaxation times on temperature and the relaxing variable itself. The models proposed by Narayanaswamy [1] and Moynihan et al. [2] (called here the NM model) and Scherer [3] and then Hodge [4] have been extensively applied to the description of the structural relaxation of polymers and other amorphous materials. In this work we will make use of the model proposed in Ref. [5, 6], which we will call hereafter the SC model. The main equations of the

model are included in the Appendix. The comparison between the experimental $c_p(T)$ curves measured after a set of distinctly different thermal histories and the model simulated thermograms allows, by means of a least-squares routine, the model parameters to be determined (three parameters called A, B and T_2 determine the temperature dependence of the relaxation times in equilibrium, the parameter β characterises the width of the distribution of relaxation times assumed to be in the form of a stretched exponential, and δ characterises the values of the configurational entropy in the limit states; all of them are material parameters independent of the thermal history). This set of parameters determines the evolution of the characteristic relaxation time, which in the SC model is assumed to obey the Adam–Gibbs equation (Eq. A3) both in equilibrium and in out-of-equilibrium states. Thus, if one accepts the model assumptions, the experimental results in the form of a set of $c_p(T)$ curves yield, through modelling, the relaxation times of the structural relaxation process.

A more direct determination of the relaxation times can be achieved by means of temperature modulated DSC (TMDSC). In this technique an oscillation or modulation of temperature is superimposed on a heating or cooling ramp at a constant rate. If the response of the material to the temperature oscillation is assumed to be linear, the measured heat flow can be expressed in the form [7]

$$\dot{q} = c_\beta \dot{T}_{av} + \omega A_T |c| \cos(\omega t - \phi) \ , \qquad (1)$$

where $\dot{T}_{av}$ is the constant rate of change of temperature in the underlying heating or cooling scan, A_T and ω are, respectively, the amplitude and angular frequency of the temperature oscillation, c_β is the apparent specific heat capacity, c is the complex heat capacity $c = c' + ic''[i = (-1)^{1/2}]$ and ϕ is the phase angle, $\tan\phi = c''/c'$. In a modulated heating scan c_β looks like the trace of a conventional DSC heating scan, showing the characteristic peaks when the sample has been previously annealed isothermally at temperatures below the glass transition, c' shows a step in the glass transition, while both c'' and ϕ show a peak. The inverse of the frequency of the temperature oscillation has been interpreted as the relaxation time τ at the temperature at which c'' or ϕ attain the maximum [8], or in terms of the modulation period $(t_p)\tau = t_p/2\pi$.

Hutchinson and Montserrat [9–11] analysed the TMDSC experiment using a model with a single relaxation time, and studied the dependence of the calculated heat flow on the characteristics of the experiment. Schawe [12] proposed a different method assuming a distribution of relaxation times according to the Havriliak and Negami [13] relaxation function with constant shape but shifting with temperature and fictive temperature along the thermal profile of the experiment.

In this work, the set of material parameters of the SC model is calculated by curve-fitting to a series of DSC heating scans. This set of parameters is assumed to describe the structural relaxation of polystyrene (PS). The model is then used to simulate the response of the material to the TMDSC experiment and the calculated result is compared with the experimental result.

Experimental

The sample was a PS molecular-weight standard (M_w = 410000, $M_w/M_n = 1.05$) from Polysciences. A single 5 mg encapsulated sample was used in all the experiments. All the thermal treatments were carried out in the calorimeter. A Pyris 1 Perkin-Elmer DSC was used for conventional and modulated calorimetry. A Perkin-Elmer DSC4 calorimeter was also used in some conventional DSC measurements. In the TMDSC heating experiments the sample was subjected to a thermal treatment that started at 423 K and included cooling at 40 K/min until the annealing temperature T_a, an isothermal stage at this temperature for t_a min, and further cooling at 40 K/min until 323 K; then, the modulated scan followed, in which a saw tooth with a period of 12 sec and an amplitude of 0.375 K was superimposed on a 2.5 K/min heating ramp. A series of TMDSC cooling experiments was performed with different periods of 12, 24 and 60 s. Immediately before each TMDSC experiment a base line using two empty aluminium pans and the same modulated thermal profile was recorded. The base line was subtracted from the heat flow measured in the experiment with the PS sample.

The measured heat flow and the sample temperature as a function of time were Fourier-analysed. The first harmonic was considered. One value of c_β, c', and of the phase angle ϕ was calculated in each cycle.

No absolute values of c' were calculated. For the purposes of the analysis of the glass transition in this work it is enough to obtain a normalised $c'(T)$ function calculated as

$$c'_N = \frac{c' - c'_g}{c'_l - c'_g} \ , \qquad (2)$$

where c'_l and c'_g are the values obtained for c' in temperature intervals corresponding to the equilibrium liquid (between 390 and 423 K in our calculations) and the glass (between 323 and 353 K). An analogous procedure was applied to obtain a normalised function $c_{\beta N}(T)$.

The phase angle has been shifted to zero at the lowest temperatures of the TMDSC experiment. Phase-angle correction was applied, following Ref. [14] to take into account the phase angle introduced by the change in the heat transfer conditions between the sample and the sample holder when going from the glass to the equilibrium liquid during the experiment.

The thermal treatments previous to the conventional DSC heating scans were as described previously for the TMDSC experiments. A series of DSC heating scans was performed after cooling the sample from 423 to 323 K at different cooling rates. The sample after cooling at 40 K/min from 423 to 323 K is called hereafter the unannealed sample. The heating rate in the DSC experiments was always 10 K/min. No absolute values of $c_p(T)$ were calculated; instead, the normalised heat flow, $\dot{Q}/m\dot{T}$, which has heat-capacity units, was determined.

Results and discussion

Conventional DSC

The heating thermograms measured after cooling the sample at different cooling rates, q_c, ranging between 0.5

and 40 K/min were used to determine the dependence of the equilibrium relaxation times on temperature according to the well-known formula [15]

$$\frac{\partial \ln\ \tau^{eq}}{\partial 1/T} = -\frac{\partial \ln q_c}{\partial 1/T_{f'}} = \frac{\Delta h^*}{R} \quad , \tag{3}$$

where $T_{f'}$ is the fictive temperature in the glassy state, i.e., the glass-transition temperature determined from the intersection of the enthalpy lines corresponding to the equilibrium liquid and to the glassy states. The values of $T_{f'}$ are shown in Fig. 1. A value of $\Delta h^*/R = 150\,\mathrm{kK}$ was found. It is difficult to compare the result with the values reported in the literature because of the great differences found among the different PS samples and methods of evaluation. Reported values for $\Delta h^*/R$ in the case of polydispherse samples range between 70 and 100 kK [4, 16–19]; nevertheless, Hodge and Huvard [16] reported a value of 175 kK evaluating data from Chen and Wang [20] obtained with a monodisperse PS. In contrast Hutchinson [21], also with a monodisperse sample, found $\Delta h^*/R = 70$ kK. The high value of Δh^* can be related to the fact that the glass-transition-temperature interval is particularly narrow in our sample. Figure 2 shows the thermogram obtained after cooling at 40 K/min from which a measure of the width of the glass transition of only $\Delta T = 4.5\,\mathrm{K}$ can be obtained (the definition of ΔT is shown in Fig. 2). The narrow temperature interval of the glass transition means that the relaxation times change very quickly with temperature, hence the high value of Δh^*.

The thermograms measured after different thermal histories are shown in Fig. 3. The model calculations were carried out with $B = 1000\,\mathrm{J/g}$. In Ref. [22] it was shown that the curve characterising the temperature dependence of the equilibrium relaxation times depends only slightly on the value of B fixed in the least-squares-fitting routine. The value of $B = 1000\,\mathrm{J/g}$ was selected for PS guided by the physical significance of the set of parameters. The solid lines correspond to the model calculation with the set of parameters found by the least-squares routine: $T_2 = 320.9\,\mathrm{K}$, $\ln A = -55.2\,\mathrm{s}$, $\beta = 0.49$, $\delta = 0.14$, a set of parameter values which is close to the one found in Ref. [22] for a PS of lower molecular weight. As shown in Fig. 3, the model is not able to predict several specific details of the experimental data, such as the small peak appearing in the thermogram of Fig. 3. It is important to note that this does not mean that the model has a particular difficulty in reproducing the thermograms measured after this thermal history: the simultaneous least-squares fit gives the set of parameters for which the overall approach of the seven calculated curves to the experimental ones is the best, and probably the contribution of the error function of this particular history is smaller than in the other ones because the values of the heat flow in the region of the peak are much smaller in this curve than after annealing or slow cooling. Nevertheless the overall fit is good taking into account that all the thermal histories are reproduced with the same set of parameters. It can be said that this set of five parameters contains all the

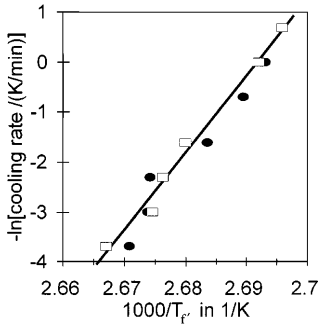

Fig. 1 Dependence of the glass-transition temperature on the cooling rate in the formation of the glass

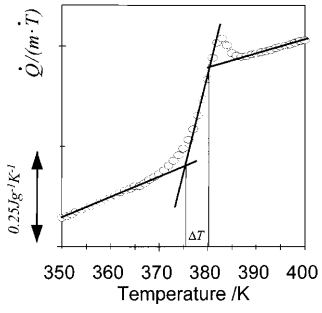

Fig. 2 Differential scanning calorimetry (*DSC*) thermogram measured after cooling at 40 °C/min. The glass-transition temperature interval ΔT is defined in the figure

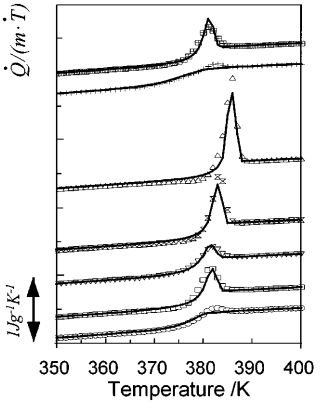

Fig. 3 Experimental results of DSC heating scans measured after different thermal histories: cooling rate 40 °C/min (○); cooling rate 0.5 °C/min (□), 100 °C for 3000 min (▽); annealing at 90 °C for 3000 min (⧖); annealing at 90 °C for 300 min (△); annealing at 70 °C for 3000 min (+); annealing at 90 °C for 300 min (⊞). The *solid line* represents the model calculation

information needed for a good approximation of the structural relaxation behaviour of this polymer.

In particular, it is possible to simulate with the model equations the evolution of the characteristic relaxation time during any of the thermal histories. The temperature dependence of the relaxation time (τ in A2, A3) during the heating scan that follows cooling at 40 K/min from equilibrium is shown in Fig. 4. At the beginning of the scan, at the lowest temperatures, the trace corresponds to an Arrhenius behaviour, with a linear dependence of $\log\tau$ on the reciprocal of temperature. The slope in this diagram permits the calculation of an apparent activation energy, E_A^{glass}, defined by

$$\frac{\partial \ln \tau^{glass}}{\partial 1/T} = \frac{E_A^{glass}}{R} \quad . \tag{4}$$

The model simulation yields a value $E_A^{glass}/R = 21$ kK. In the NM method, the relaxation time is a function of both the temperature and the fictive temperature through

$$\tau = \tau_0 \exp\left[\frac{\Delta h^*_{NM}}{R}\left(\frac{x}{T} + \frac{1-x}{T_f}\right)\right] \quad . \tag{5}$$

Taking into account that at equilibrium $T_f = T$ and in the glassy state $T_f = T_{f'}$, which is independent of temperature, one can identify $\Delta h^* = \Delta h^*_{NM}$ and then

$$\frac{\partial \ln \tau^{glass}}{\partial 1/T} = \frac{E_A^{glass}}{R} = \frac{x\Delta h^*_{NM}}{R} \quad . \tag{6}$$

Thus, the set of parameters determined from the experimental thermograms allows a value of $x = 0.15$ to be determined through the model simulation. It is difficult to extract a value of the parameter x of PS from the literature due to the fact that when the NM method has been applied to experimental DSC results with a curve-fitting procedure it was necessary to use very different values of the parameters for the different thermal histories. Hodge [4] gave a value of $x = 0.48$ by curve-fitting with $\Delta h^*/R = 78$ kK. Hutchinson [21] applied the peak-shift method to determine x as a material parameter, independent of the thermal history, and found a value of $x = 0.46$ for a PS in which $\Delta h^*/R = 70$ kK. A correlation between x and Δh^* in the NM model [23, 24] has been pointed out. High values of the latter parameter correspond to low values of the x parameter. Hodge and Huvard [16] reported a value of $x = 0.12$ for a sample with $\Delta h^*/R = 175$ kK. The low value of x in our sample must be related to the high value of Δh^* and the narrow glass-transition-temperature interval.

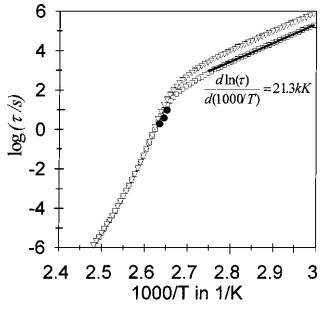

Fig. 4 Relaxation time (τ in Eq. A2) obtained by model simulation of a heating scan carried out after cooling the sample at 40 °C/min from the equilibrium liquid. (The *squares* show the results of the calculations carried out with $B = 1000$ J/g, $T_2 = 320.9$ K, $\ln A = -55.2$ s, $\beta = 0.49$ and $\delta = 0.14$; the *triangles* represent the result of the model simulation with the same values of B, T_2, $\ln A$ and β but with $\delta = 0$, see text.) The *filled circles* are the relaxation times obtained from the temperature-modulated DSC (*TMDSC*) results shown in Fig. 5

The approach from the glassy to the equilibrium behaviour occurs around the glass transition and at higher temperatures the temperature dependence of the relaxation time is given by the equilibrium equation

$$\tau^{eq}(T) = A \exp\left(\frac{B}{TS_c^{eq}(T)}\right) \quad . \tag{7}$$

When the slope of the equilibrium line is calculated from the model simulation at the glass-transition temperature (T_g)

$$\frac{\partial \ln \tau^{eq}}{\partial 1/T}(T_g) = 150\,\text{kK} \tag{8}$$

is found, in good agreement with the experimental one given by Eq. (3).

The role played in the kinetics of the structural relaxation process by the fact that the configurational entropy in the limit state which would be attained at infinite time is higher than the extrapolated equilibrium entropy can be clarified by looking at the relaxation times calculated by computer simulation. In Fig. 4 the temperature dependence of the relaxation time during the heating scan that follows cooling at 40 °C/min calculated with the model equations and the set of parameters found by the search routine are compared with that calculated with the same values of $B, \ln A, T_2$ and β, but with $\delta = 0$. The latter correspond to a structural relaxation process that attains the extrapolated equilibrium state at infinite time, i.e., $S_c^{lim}(T) = S_c^{eq}(T)$. In that case, clearly, the relaxation times in the glassy state are higher than the relaxation times which correctly reproduce the experimental results, although the apparent activation energy is almost equal in both simulations. This can be interpreted in the sense that the mobility in the glassy states attained after quick cooling from temperatures higher than the glass transition is actually higher than what it would be if the evolution of the structural relaxation had the extrapolated equilibrium state as the limit at infinite time. This feature is also related to the kinetics of the structural relaxation process: as a consequence of the difference between $S_c^{lim}(T)$ and $S_c^{eq}(T)$ in the relaxation process, the cooling

yields states with higher configurational entropies and thus smaller relaxation times than if $S_c^{lim}(T) = S_c^{eq}(T)$. Clearly the value of the δ parameter does not affect the value of the relaxation times at temperatures above the glass transition. From a phenomenological point of view this makes the relaxation rate higher in the glassy state and gives the model the ability to reproduce simultaneously, with the same set of parameters, the $c_p(T)$ curves measured after different thermal histories. The molecular interpretation of this behaviour rests on the interpretation of the difference between $S_c^{lim}(T)$ and $S_c^{eq}(T)$, through the collapse of the conformational mobility when the number of available conformational states attains a critical value which is still higher than the one corresponding to equilibrium.

As a conclusion it can be said that modelling the DSC conventional thermograms obtained with a broad enough set of thermal histories allows the characterisation of the structural relaxation process in which all the information needed is contained in a set of five material parameters. These parameters can be used to get a quite consistent picture of the evolution of the relaxation time of the conformational motions of the main chain segments in response to different thermal histories.

Results of TMDSC

Figure 5 shows c'_N and ϕ as a function of temperature for three modulated cooling scans with frequencies of 0.083, 0.042 and 0.017 Hz, showing the shift of the dynamic glass transition towards lower temperatures as the frequency decreases. If, as is frequently done in dielectric or dynamic mechanical relaxation spectroscopies, it is assumed that the phase angle goes through a maximum at a temperature such that the characteristic relaxation time is $\tau = 1/(2\pi f)$, with f the frequency of temperature oscillation, then the position of the maximum of the phase angle in Fig. 5 can be used to obtain three points in the $\log(\tau)$ versus $1/T$ plot of Fig. 4. The agreement with the results obtained from conventional DSC is quite clear. The points obtained from the TMDSC experiments fall on the part of the $\log(\tau)$ versus T curve which corresponds to the temperature interval just above the glass transition. This is an indication of the separation of the dynamic response (corresponding to the oscillation) and the essentially nonlinear response corresponding to the underlying thermal profile.

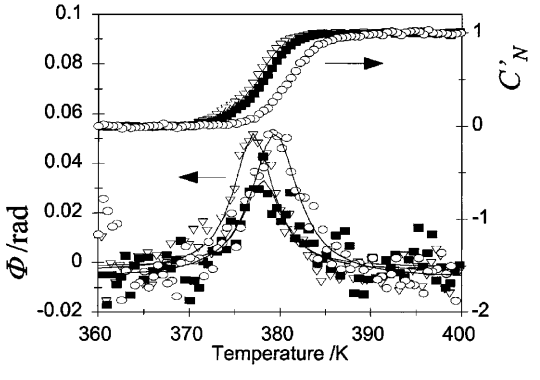

Fig. 5 Temperature dependence of the normalised c'_N and the phase angle ϕ obtained from TMDSC cooling experiments with different periods: 12 s (○), 24 s (■), 60 s (▽)

Modulated heating scans were performed after thermal treatments that included annealing for 1000 min at 343 and 363 K and on the unannealed sample. The results are presented in Fig. 6. The $c_\beta(T)$ curves have the same trend as the $c_p(T)$ ones. The curve obtained after annealing at 363 K shows a great peak whose maximum appears at a temperature higher than T_g (Fig. 6) while, after annealing at 343 K, $c_\beta(T)$ shows a sub-T_g peak appearing as a shoulder in the low temperature region of the glass transition (Fig. 6). This shoulder also appears in the heat-flow curve measured after the same thermal treatment in conventional DSC (Fig. 3). The $c_\beta(T)$ curve measured on the unannealed sample (Fig. 6) shows a small peak on the high-temperature side of the transition, as happens in the DSC thermogram (Fig. 3).

The dynamic glass transition covers a temperature interval much narrower after annealing at 363 K (Fig. 7A) than in the unannealed sample (Fig. 7B), as shown in the $c'_N(T)$ and $\phi(T)$ curves. In the temperature interval immediately below the transition step both c'_N and ϕ take values below those corresponding to the glassy state (which have been taken arbitrarily to be zero for both functions). This feature has been found by several authors both experimentally [7, 11] and through model simulation [11]. The temperature at which the phase angle goes through the maximum also changes slightly. In the heating scan measured on the unannealed sample it is 380.2 K and after annealing at 363 K for 1000 min it appears at 381.0 K. In contrast, after annealing at 343 K the $c'_N(T)$ and $\phi(T)$ curves are not distinguishable from those of the unannealed sample within the experimental accuracy (results not shown).

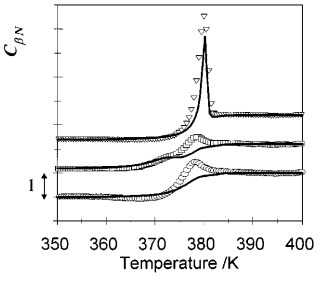

Fig. 6 Temperature dependence of $c_{\beta N}$ measured in the unannealed sample (○), after annealing at 90 °C for 1000 min (□) and after annealing at 70 °C for 1000 min (▽). The *open symbols* represent the values calculated from the experimental results and the *solid line* the ones obtained by computer simulation

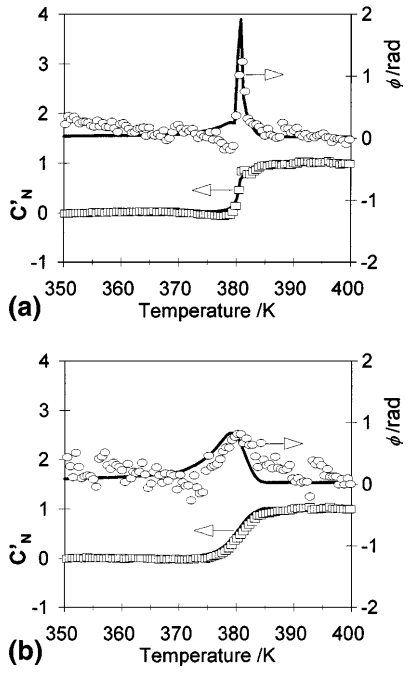

Fig. 7 Temperature dependence of c' and the phase angle ϕ obtained from TMDSC in heating scans measured **a** after annealing at 90 °C for 1000 min, and **b** in the unannealed sample

Computer simulation of the TMDSC experiments used the same equations as the calculations done for conventional DSC. The actual thermal profile was simulated by a series of temperature jumps followed by isothermal periods (eight in each cycle) such that at the end of each step the temperature attains the point corresponding to the superposition of a sinusoidal oscillation of the same amplitude and period as the experimental saw tooth superposed on the underlying ramp. The model equations provide the value of the configurational entropy (Eq. A1) and enthalpy (Eq. A9) during the whole stepped thermal history, in particular, at the end of each step. In this way eight data points of the heat flow per cycle are obtained. Fourier analysis of this curve allows the calculation of the model simulated $c_\beta(T)$, $c'_N(T)$ and $\phi(T)$ curves, which are represented in Figs. 6 and 7 by the solid lines. No curve-fitting was performed, and the model calculations used the set of material parameters determined from the DSC scans reported in the previous section.

The agreement between experiment and model simulation is quite good in the case of the $c'_N(T)$ and $\phi(T)$ curves. The main features are well reproduced by the model, including the different width of the transition in the unannealed sample and after annealing at 363 K. The shift of the peak maximum with annealing is also qualitatively reproduced, but in the model calculation the predicted shift is 1.6 K, which is larger than the experimental value of 0.8 K. In the case of $c_\beta(T)$ curves the fit of the unannealed sample has the same shortcoming as in the conventional DSC trace, namely the small overshoot is not reproduced by the model equations. The curve calculated for the thermal treatment that includes annealing at 343 K has the same problem in that the overshoot is not reproduced, but the sub-T_g peak appears clearly in the model simulated trace. The peak in the curve calculated for the sample annealed at 363 K is quite close to the experimental one.

Concluding remarks

We have shown that the results of conventional DSC and TMDSC experiments in the glass-transition region can be analysed based on the same physical concepts and can be modelled with the same phenomenological equations.

The possibility of separating the reponse to the TMDSC thermal history into a linear response to the temperature oscillation, i.e., a dynamic glass transition characterised by the fuctions $c'(T)$ and $\phi(T)$, and a nonlinear response to the underlying heating or cooling scan characterised by c_β, comes from the fact that the former are mainly due to the equilibrium calorimetric relaxation times (which fall in the equilibrium part of the $\log\tau$ versus $1/T$ plot), while c_β depends on the whole thermal history of the experiment.

Anyway, $c'(T)$ and $\phi(T)$ depend on the thermal history. Previous annealing at a temperature below the glass transition but close to T_g produces a change in the width of the temperature interval in which the dynamic glass transition takes place with a small shift in the position of the maximum. The model simulation reproduces these features correctly.

Acknowledgement This work was supported by CICYT through the CICYT MAT97-0634-C02-01 project.

Appendix

The evolution of the configurational entropy during a thermal history that consists of a series of temperature jumps from T_{i-1} to T_i at time instant t_i followed by isothermal stages is given by

$$S_c(t) = S_c^{\lim}[T(t)] - \sum_{i=1}^{n}\left(\int_{T_{i-1}}^{T_i}\frac{\Delta c_p^{\lim}(T)}{T}\mathrm{d}T\right)\phi(\xi-\xi_{i-1}) \quad , \tag{A1}$$

where ξ is the reduced time

$$\xi = \int_0^t \frac{\mathrm{d}t'}{\tau(t')} \quad . \tag{A2}$$

The function $\tau(t)$ is determined implicitly by the dependence of τ on T and S_c during the thermal history,

a dependence which is assumed to obey the equation of Adam and Gibbs extended to nonequilibrium states:

$$\tau(T, S_c) = A \exp\left(\frac{B}{TS_c(\xi, T)}\right) \tag{A3}$$

and the relaxation function is assumed to be a stretched exponential of the reduced time:

$$\phi(\xi) = \exp(-\xi^{\beta}) \ . \tag{A4}$$

$S_c^{lim}(T)$ represents the value of the configurational entropy attained in the physical ageing process at infinite time, and $\Delta c_p^{lim}(T)$ is defined through

$$S_c^{lim}(T_i) - S_c^{lim}(T_{i-1}) = \int_{T_{i-1}}^{T_i} \frac{\Delta c_p^{lim}(T)}{T} dT \ . \tag{A5}$$

Thus, if T^* is a temperature above the glass-transition region, for any temperature T, in the glass-transition temperature interval or below it,

$$S_c^{lim}(T) = S_c^{eq}(T^*) + \int_{T^*}^{T} \frac{\Delta c_p^{lim}(T)}{T} dT \ , \tag{A6}$$

with

$$S_c^{eq}(T) = \int_{T_2}^{T} \frac{\Delta c_p(T)}{T} dT \tag{A7}$$

where $\Delta c_p(T)$ is the conformational heat capacity, taken here as the difference between the heat capacities of the liquid and the glass, $\Delta c_p(T) = c_{pl}(T) - c_{pg}(T)$ [a linear dependence of $\Delta c_p(T)$ with temperature has been assumed in this work] and T_2 is the Gibbs–DiMarzio temperature at which the configurational entropy in the equilibrium liquid would vanish.

The phenomenological models of the structural relaxation usually assume that the state attained at infinite time in the structural relaxation process at a temperature T_a can be identified with the extrapolation to T_a of the equilibrium line experimentally determined at temperatures above T_g [1–4]. When the models are based on the fictive temperature concept T_f this is simply a result of the identification of the limit of T_f at infinite time with T. In the context of the SC model this means that

$$S_c^{lim}(T) = S_c^{eq}(T) \ . \tag{A8}$$

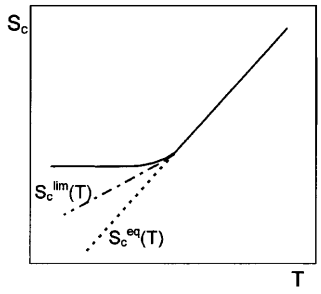

Fig. 8 Sketch of the configurational entropy corresponding to the liquid state (*dashed line*), to an experimental cooling scan at a finite cooling rate (*solid line*), and to the hypothetical line of the limit states of the structural relaxation process (*dashed-dotted line*)

However, it has been shown that the agreement between the model simulation and the experiments is highly improved when the model includes an assumption leading to values of $S_c^{lim}(T)$ significantly higher than those of $S_c^{eq}(T)$, and the results in this work also support this idea. The definition of the curve $S_c^{lim}(T)$ introduces new adjustable parameters into the model. The shape shown in Fig. 8 has been chosen because it needs only one additional parameter, δ.

The model is compared with the experimental results of conventional DSC through its prediction of the heat capacity as a function of temperature during the measuring scan or, with TMDSC results, through the prediction of the heat flow as a function of time. In both cases the evolution of configurational enthalpy with time along the whole thermal history has to be calculated from the model equations. This is done with the assumption that configurational enthalpy and entropy have the same relaxation function which yields the following equation for configurational enthalpy:

$$H_c(t) = H_c^{lim}[T(t)] - \sum_{i=1}^{n} \left[\int_{T_{i-1}}^{T_i} \Delta c_p^{lim}(T) dT\right] \times \exp\left[-\left(\int_{t_{i-1}}^{t} \frac{d\sigma}{\tau(\sigma)}\right)^{\beta}\right] \ . \tag{A9}$$

References

1. Narayanaswamy OS (1971) J Am Ceram Soc 54: 491
2. Moynihan CT, Macedo PB, Montrose CJ, Gupta PK, DeBolt MA, Dill JF, Dom BE, Drake PW, Esteal AJ, Elterman PB, Moeller RP, Sasabe H (1976) Ann NY Acad Sci 279: 15
3. Scherer GW (1984) J Am Ceram Soc 67: 504
4. Hodge IM (1987) Macromolecules 20: 2897
5. Gómez Ribelles JL, Monleón Pradas M (1995) Macromolecules 28: 5867
6. Gómez Ribelles JL, Monleón Pradas M, Vidaurre Garayo A, Romero Colomer F, Más Estellés J, Meseguer Dueñas JM (1997) Polymer 38: 963
7. Schawe JEK (1995) Thermochim Acta 261: 183
8. Weyer S, Hensel A, Korus J, Donth E, Schick C (1997) Thermochim Acta 304/305: 251

9. Hutchinson JM, Montserrat S (1996) J Therm Anal 47: 163
10. Hutchinson JM, Montserrat S (1996) Thermochim Acta 286: 263
11. Hutchinson JM, Montserrat S (1997) Thermochim Acta 304/305: 257
12. Schawe JEK (1998) J Polym Sci Polym Phys Ed 36: 2165
13. Havriliak S, Negami S (1966) J Polym Sci C 14: 99
14. Weyer S, Hensel A, Schick C (1997) Thermochim Acta 304/305: 267
15. Mohynihan CT, Esteal AJ, DeBolt MA, Tcker J (1976) J Am Ceram Soc 59: 12
16. Hodge IM, Huvard GS (1983) Macromolecules 16: 371
17. Hodge IM (1994) J Non-Cryst Solids 169: 211
18. O'Reilly JM, Hodge IM (1991) J Non-Cryst Solids 131–133: 451
19. Privalko VP, Demchenko SS, Lipatov YS (1986) Macromolecules 19: 901
20. Chen HS, Wang TT (1981) J Appl Phys 52: 5898
21. Hutchinson JM (1992) Prog Colloid Polym Sci 87: 69
22. Brunacci A, Cowie JMG, Ferguson R, Gómez Ribelles JMG, Vidaurre Garayo A (1996) Macromolecules 29: 7976
23. Hodge IM (1991) J Non-Cryst Solids 131–133: 435
24. Cortés P, Montserrat S (1998) J Polym Sci Part B Polym Phys 36: 113